Deriving C_4 photosynthesis parameters by fitting intensive A/C_i curves

Haoran Zhou[1], Erol Akçay and Brent Helliker

Department of Biology, University of Pennsylvania, PA19104

Corresponding author: Haoran Zhou

Address: 433 S University Ave. 314 Leidy Labs,

Department of Biology, University of Pennsylvania, PA19104

Email: haoranzh@sas.upenn.edu

Running title: Deriving C_4 photosynthesis parameters

Received _____; accepted _____

ABSTRACT

Photosynthetic assimilation versus intercellular CO_2 response curves (A/C_i) are widely measured to estimate photosynthetic parameters for C_3 species; however, few parameters have been reported for C_4 because of lacking estimation methods. In the current study, we took the frameworks of widely-used estimation methods for C_3 and built estimation tools to fit intensive A/C_i curves (6-8 more sampling points) for C_4 based on two different assumptions about photosynthesis models and two fitting procedures with estimation improvements. Five photosynthetic parameters are obtained: maximal Rubisco carboxylation rate (V_{cmax}), electron transport rate (J), day respiration (R_d), maximal PEPc carboxylation rate (V_{pmax}) and mesophyll conductance (g_m). Simulation tests with random errors, out of sample tests and Chlorophyll fluorescence measurements validated the estimation methods. Sensitivity analysis showed V_{cmax}, J and V_{pmax} are robust to variation in the input parameters, while R_d and g_m varied. The two photosynthesis model assumptions yielded consistent results, although they are different from each other in whether ATP could freely transport between RuBP regeneration and PEP regeneration processes. For the two fitting procedures, one is preferable (lower estimation error) if additional measurements (e.g. fluorescence) are available, however, the two procedures support each other and we recommend using both to achieve more accurate results.

Subject headings: C_4, photosynthesis parameters,A/Ci curves, nonlinear curve fitting

INTRODUCTION

Key photosynthetic parameters allow for the assessment of how biochemical and biophysical components of photosynthesis affect net carbon assimilation in response to environmental changes, genotypic differences and genetic modification. The changes in net assimilation (A) that occur along with the changes of intercellular CO_2 concentration (C_i) —or A/C_i curves— are widely used to fit photosynthetic parameters for C_3 species. Sharkey et al. (2007) developed a method for estimating photosynthesis parameters of C_3 species using the C_3 photosynthesis model of Farquhar et al. (1980; FvCB model), that has been one of the most widely used tools since it is based exclusively on A/C_i curves, which are easy to measure in both lab and field conditions.

Fewer estimates of photosynthetic parameters have been reported for C_4 species, as there has been a lack of accessible C_4 estimation methods. Several recent studies, however, used A/C_i curves to estimate C_4 photosynthesis parameters (Yin et al. 2011b; Ubierna et al. 2013; Bellasio et al. 2015). These studies usually use partial A/C_i curves; measuring assimilation rates for only a few CO_2 concentrations coupled to ancillary measurements of chlorophyll fluorescence and/or 2 % O_2. While these estimation methods lead to good estimates of photosynthetic parameters, the additional measurement requirements make estimation more cumbersome for field work or large-scale sampling.

Gu et al. (2010) have pointed out several issues with previous estimation methods using A/C_i curves. First, the structure of the FvCB model makes it easy to be over-parameterized. Second, a general shortcoming for both C_3 and C_4 estimation methods, is that they require an artificial assignment of the RuBP regeneration and Rubisco carboxylation limitation states for the

A/C_i (Xu & Baldocchi 2003; Ethier et al. 2006; Ubierna et al. 2013; Bellasio et al. 2015), which has turned out to be problematic (Type I methods). These methods assume constant transition points of limitation states for different species. Furthermore, Type I methods tend to minimize separate cost functions of different limitation states instead of minimizing a joint cost function. Some recent estimation methods ameliorate these problems by allowing the limitation states to vary at each iterative step of minimizing the cost function (Type II methods; Dubois et al. 2007; Miao et al. 2009; Yin et al. 2009; Gu et al. 2010). However, for these type II methods, additional degrees of freedom in these "auto-identifying" strategies can lead to over-parameterization if limitation states are allowed to change freely for all data points. Gu et al. (2010) also pointed out that existing Type I and Type II methods fail to check for inadmissible fits, which happen when estimated parameters lead to an inconsistent identification of limitation states from the formerly assigned limitation states.

Theoretically, it is possible to estimate photosynthetic parameters for C_4 species by exclusively fitting A/C_i curves to a C_4 photosynthesis model, but such approaches encounter two problems. First, at low C_i, the slope of A/C_i is very steep and the assimilation rate saturates quickly. Second, C_4 species have more photosynthetic parameters as the carbon concentrating mechanism adds complexity. Here we present a A/C_i-based C_4 parameter estimation protocol that is solely A/C_i-based, and attempts to solve the general problems and drawbacks outlined above.

We extend the framework of Sharkey et al. (2007) to estimate photosynthetic parameters for C_4 species based on intensive A/C_i curves (A/C_i curves with 6-8 more sampling points than the common A/C_i for C_3 species), examine two different assumptions about the ATP, one

product of electron transport, distribution between RuBP regeneration and PEP regeneration in C_4 photosynthesis models and further examine two separate fitting procedures. We estimate the five photosynthesis parameters: (1) maximum carboxylation rate allowed by ribulose 1,5-bisphosphate carboxylase/oxygenase (Rubisco) (V_{cmax}), (2) rate of photosynthetic electron transport (J), (3) day respiration (R_d), (4) maximal PEPc carboxylation rate (V_{pmax}), and (5) mesophyll conductance (g_m). This approach yields the following improvements to eliminate common problems occurring in previous C_3 and C_4 estimation methods: avoiding over-parameterization, maximizing joint cost function, freely determining transition points instead of assigning in advance, and checking for inadmissible fits.

THE MODEL

Diffusion processes

In the C_4 photosynthesis pathway, the enzyme PEPc first fixes CO_2 into C_4 compound and then, releases CO_2 into bundle sheath cells, where photosynthesis reactions of C_3 cycle occur. The diffusion of CO_2 starts from ambient atmosphere through stomata into intercellular spaces, then into the mesophyll cells, finally into the bundle sheath cells. The A/C_i curves give the intercellular CO_2 concentration (C_i). Thus, in our model, we need to further consider the CO_2 concentration in mesophyll cells (C_m, eq. (1)) and the CO_2 concentration in bundle sheath cells (C_{bs}, eq. (2)). C_m is determined by four processes as follows: the diffusion of CO_2 from the intercellular space (C_i) to mesophyll through mesophyll plasma membrane, the fixation of CO_2 by PEP carboxylation (V_p), bundle sheath leakage from bundle sheath cells back to mesophyll ($g_{bs}(C_{bs} - C_m)$) and mitochondrial respiration rate at daytime in mesophyll cells (R_{dm}). C_{bs} is

determined by PEP carboxylation (V_p), bundle sheath leakage gross assimilation and daytime mitochondrial respiration rate in bundle sheath cells (R_{dbs}). The total daytime respiration (R_d) is the sum of R_{dm} and R_{dbs} (eq. (3)).

$$\frac{\partial C_m}{\partial t} = (C_i - C_m)g_m - [V_p - g_{bs}(C_{bs} - C_m)] + R_{dm} \tag{1}$$

$$\frac{\partial C_{bs}}{\partial t} = V_p - g_{bs}(C_{bs} - C_m) - A_g + R_{dbs} \tag{2}$$

$$R_d = R_{dbs} + R_{dm}, \tag{3}$$

where g_m is the mesophyll conductance, $g_{bs}$is the bundle sheath conductance for CO_2 and A_g is the gross assimilation rate. We assume the whole system is in the steady state and set the right-hand sides of eq. (1) and (2) equal to zero. The net assimilation rate A_n is equal to $A_g - R_d$. Then, at equilibrium,

$$A_n = V_p - g_{bs}(C_{bs} - C_m) - R_{dm} \tag{4}$$

$$A_n = (C_i - C_m)g_m\ . \tag{5}$$

Next, we consider the O_2 in the bundle sheath cells (O_{bs}).

$$\frac{\partial O_{bs}}{\partial t} = \alpha A_g - g_{bso}(O_{bs} - O_m) \tag{6}$$

$$g_{bso} = g_{bs}\frac{D_{o_2}S_{o_2}}{D_{co_2}S_{co_2}}, \tag{7}$$

where g_{bso} is the bundle sheath conductance for O_2, O_m is the O_2 concentration at mesophyll cell and α ($0 < \alpha < 1$) denotes the fraction of O_2 evolution occurring in the bundle sheath. D_{o_2} and D_{co_2} are the diffusivities for O_2 and CO_2 in water and S_{o_2} and S_{co_2} are the Henry constants, which gives

$$g_{bso} = 0.047 g_{bs}. \tag{8}$$

At equilibrium, eq. (6) =0. And we have:

$$O_{bs} = \frac{\alpha A_g}{0.047 g_{bs}} + O_m. \tag{9}$$

Here we assume O_m=O_a, which is the ambient O_2 concentration, as is done in other studies (von Caemmerer 2000; Yin et al. 2011b). Eq. (9) indicates that O_2 will accumulate in the bundle sheath. If α=0, then, O_{bs}=O_m=O_a. With a α >0, O_{bs} is higher than O_m or O_a, because the bundle sheath is a gas-tight compartment (low g_{bs}) that prevents the O_2 produced by photosynthesis from diffusing out of the cells.

PEP carboxylation

PEP carboxylation is limited either by PEPc reaction rate (V_{pc}) or PEP regeneration (V_{pr}). V_{pc} follows a Michaelis-Menten equation:

$$V_{pc} = \frac{V_{pmax} C_m}{C_m + K_p}, \tag{10}$$

where V_{pmax} is the maximum PEPc carboxylation rate and K_p is the Michaelis-Menten coefficient of CO_2. V_p usually is assumed to have an upper bound (V_{pr}) set by PEP regeneration rate:

$$V_p = \min\left(V_{pc}, V_{pr}\right). \tag{11}$$

FvCB model for the C_3 cycle

A_n represents the assimilation rate by the C_3 cycle of the C_4 photosynthesis pathway, thus it can be modeled by a modified FvCB model of C_3 photosynthesis (Farquhar et al. 1980). In this model, A_n is given by one of two equations, each corresponding to limitation by a different reaction. The first is the Rubisco carboxylation limited state(A_c), when there's a saturating supply

of the substrate (RuBP) for Rubisco and the reaction rate is given by the enzyme kinetics of Rubisco. This normally occurs when the CO_2 concentration is low. The second is the RuBP regeneration limited state(A_j), which normally indicates the electron transport limitation in the light reaction of photosynthesis. The FvCB model computes A separately for each of the two states and takes the minimum of them to be the net assimilation rate.

The assimilation rate under Rubisco carboxylation rate, A_c, of C_4 species can be modeled as

$$A_c = \frac{V_{cmax}(C_{bs} - \gamma^* O_{bs})}{C_{bs} + K_c(1 + \frac{O_{bs}}{K_o})} - R_d, \tag{12}$$

$$\gamma^* = \frac{V_{omax} K_c}{V_{cmax} K_o}, \tag{13}$$

where V_{omax} is the maximum oxygenation rate allowed by Rubisco. The parameter γ^* represents the specificity of Rubisco and is considered as a constant given temperature among C_4 species.

When modeling the RuBP regeneration limited assimilation rate, A_j, we need to take into account the cost of C_4 photosynthesis pathway into consideration. The cost of C_4 photosynthesis stems from the 2 additional ATP/CO_2 in PEPc carboxylation and regeneration. The ATP cost come out of the electron transport of the light reactions (Hatch, 1987). This cost will be reflected in the A_j and V_{pr}. V_{pr} in eq. (11) is defined as proportional to electron transport rate (J),

$$V_{pr} = xJ/2, \tag{14}$$

where x is the fraction of total electron transport that is used for producing ATP for the PEP regeneration. The factor 1/2 accounts for the fact that when the PEPc carboxylate one molecule of CO_2, it needs 2 additional electron transport.

Then, we need to specify how ATP, or more generally electron transport, is allocated between PEP and RuBP regeneration. Two different equations based on two assumptions about electron

transport has been used in the literature to describe RuBP regeneration process in C_4 plants. In the first equation (von Caemmerer 2000), a constant proportion of electron transport is distributed for PEP carboxylation/regeneration; thus, A_j is given as follows:

$$A_j = \frac{(1-x)J(C_{bs} - \gamma^* O_{bs})}{4C_{bs} + 8\gamma^* O_{bs}} - R_d, \tag{15}$$

where the factor (1-x)/2 in the first term represents the cost of CCM in C_4 compared to the C_3 pathway. This equation assumes that no matter how much electron transport is used for PEP carboxylation/regeneration, xJ is confined for this use, thus, only (1-x) is left for RuBP regeneration (Supplementary Material I, II).

In the second equation (Vico and Porporato 2008; Osborne and Sack 2012), electron transport can be freely distributed between PEP carboxylation/regeneration and RuBP regeneration. $2V_{pr}$=xJ denotes the maximal fraction of electron transport that could be used for PEP carboxylation/regeneration instead of being confined solely for PEP carboxylation/regeneration as in the first model (Supplementary Material III). A_j is given by

$$A_j = \frac{(J - 2V_p)(C_{bs} - \gamma^* O_{bs})}{4C_{bs} + 8\gamma^* O_{bs}} - R_d, \tag{16}$$

where we deducted $2V_p$ to account for the cost of CCM in the RuBP regeneration equation.

The A_n of C_4 species is limited by two states as follows:

$$A_n = \min(A_c, A_j). \tag{17}$$

In the two models, we assumed R_{dm}=R_{dbs}, thus,

$$R_{dm} = R_{dbs} = 1/2R_d. \tag{18}$$

ESTIMATION PROTOCOL

We performed intensive A/C_i curves on nine different C_4 species to develop and examine the efficacy of our estimation tools: $Zea\ mays$ L., $Eragrostis\ trichodes$ (Nutt.) Alph. Wood, $Andropogon\ virginicus$ L., $Schizachyrium\ scoparium$ (Michx.) Nash, $Panicum\ virgatum$ L., $Panicum\ amarum$ Elliott, $Setaria\ faberi$ Herrm., $Sorghastrum\ nutans$ (L.) Nash and $Tripsacum\ dactyloides$ (L.) L. The intensive A/C_i curves measured more sample points under more CO_2 concentrations than the default curve used for C_3 species. Here we set the CO_2 concentrations as 400, 200, 50, 125, 150, 175, 200, 225, 250, 275, 300, 325, 350, 400, 500, 600, 700, 800, 1000, 1200, 1400 ppm under light intensity of 1500 $\mu molm^{-2}s^{-1}$. The data sets were obtained using LI-6400 (LI-COR Inc., Lincoln, NE, USA). If the stomatal conductance of a species does not decrease quickly at high CO_2, then the sample points at the high CO_2 level can be increased. First, we checked whether the estimation methods based on different assumptions in electron transport yielded different results. Second, we used two different fitting procedures to compare their estimation results and their advantages/disadvantages. Third, in order to test the reliability of the estimated parameters, we conducted sensitivity analyses of parameter estimates to variations in the input parameters. Finally, we conducted simulation tests using A/C_i curves generating with known parameters and added random error, out of sample test and Chlorophyll fluorescence measurement to validate the estimation methods.

We built the estimation methods using the non-linear curve-fitting routine in MS Excel and R to get solutions that minimize the squared difference between observed and predicted assimilation rates (A). There are five parameters that need to be estimated by fitting the A/C_i curve. They

are V_{cmax}, J, R_d, V_{pmax} and g_m. We are using a x with 0.4 as von Caemmerer (2000) suggested. Several studies reported robust measurements of 0.4 for different species (Ubierna et al. 2013; Yin et al. 2011b; Bellasio et al. 2015). The limitation states of assimilation rate change with C_i in A/C_i curves. Under the low C_i, photosynthesis would be limited by Rubisco carboxylation (denoted limitation: 1). Under the high C_i, photosynthesis would be limited by RuBP regeneration (denoted limitation: 2).The limitation of PEPc carboxylation and PEP regeneration has been taken into account in eq. (11).

Below is a description of the estimation process and algorithm and further details are shown in Supplementary Materials. The estimation methods are available in both Excel (Supplementary Material I and II) and R ("C4Estimation").

Input data sets and preliminary calculations

The input data sets are the leaf temperature during measurements, atmosphere pressure, two CO_2 bounds (CaL and CaH discussed in the following section), and the assimilation rates (A) and the C_is (in ppm) in the A/C_i curve. Also, reasonable initial values of output parameters need to be given in the output section. C_i will be adjusted from the unit of ppm to the unit of Pa inside the program as suggested by Sharkey et al. (2007).

Estimating limitation states

We set upper and lower limits to the value of C_i at which the assimilation transitions between limitation states, and to avoid over-parameterization, pre-assigned limitation states at the lower and upper ends of the C_i range. We assumed that under very low C_i (CaL), A is given by A_c and under very high C_i (CaH) A is given by A_j (Fig. 1). To find a suitable value for a transition point,

we suggest setting CaL as 15 Pa initially, then adjusting based on the preliminary results. The last three points can initially be set as being limited by A_j primarily (based on the three points, we can set how much CaH is) or use 65 Pa as the first trial. The points between CaL to CaH can be limited by either A_c or A_j and will be freely determined by minimizing the cost function. The range of freely determined points can be adjusted by users by setting appropriate CaL and CaH. In the column of "Estimate Limitation", whether the data points are limited by A_c (represented by "1"), A_j (represented by "2") or freely vary between A_c and A_j limitations (represented by "0") will be determined automatically by the given values of CaL and CaH. One can input "-1" to disregard a data pair. Users can adjust limitation states according to how many points and the range of C_i they have in their A/C_i curves.

Estimation algorithm and two fitting procedures

The objective of our estimation methods is to minimize the following joint cost function (eq. (22)) by varying the above five output parameters (V_{cmax}, J, V_{pmax}, R_d and g_m).

$$f = \sum_{i=1}^{n} [\text{If } (C_i < C_t),\, A = A_{ci}, \text{otherwise } A = A_{ji}) - A_{mi}]^2 \tag{19}$$

$$\text{Constraint: } CaL < C_t < CaH, \tag{20}$$

where n is the total number of observations, C_t is the intercellular CO_2 at which photosynthesis transitions from Rubisco carboxylation limited to RuBP regeneration limited, A_{ci} and A_{ji} are Rubisco carboxylation limited and RuBP regeneration limited net assimilation rate respectively, A_{mi} is the observed net assimilation rate and CaL and CaH represent the lower and upper bounds of C_t. As C_t is determined by the function of all the estimation parameters and is not easy to get

its explicit form, we use the following objective function:

$$A_i = [\text{If } (C_i \leqslant CaL), A_{ci}; \text{If } (C_i \geqslant CaH), A_{ji}; \text{If } (CaL < C_i < CaH), \min(A_{ci}, A_{ji})] \quad (21)$$

$$f = \sum_{i=1}^{n} (A_i - A_{mi})^2. \quad (22)$$

If C_i is lower than CaL, A_n will be limited by Rubisco carboxylation. If C_i is higher than CaH, A_n will be limited by RuBP regeneration. If C_i is higher than CaL and lower than CaH, A_n will be the minimum between A_{ci} and A_{ji}.

In this calculation, we take K_c, K_o, γ^*, K_p, α and g_{bs} as given (input parameters), similar to Sharkey et al. (2007), to avoid over-parameterizing the FvCB model (Gu et al. 2010). We conduct further sensitivity analyses in the following section to determine the effects of variability of these inputs parameters on the estimation results.

We used two fitting procedures in the current study: one was from Sharkey et al. (2007), which is an implicit minimization of error (Supplementary Material I), and the other one was based on the explicit calculations given by Yin et al. (2011b) (Supplementary Material II). For the method of Sharkey et al. (2007), "estimated" A_n was calculated using the above equations and observed A_n values. We call them "estimated", because when we calculate A_n, observed A_n are used to calculate some intermediate parameters, for example C_m. We calculated C_m and O_{bs} using eq. (5) and eq. (9) and two sets of V_p values using eq. (10) and eq. (14). We use the V_p value for each observation to calculate C_{bs} using eq. (4), which we then use to calculate A_c and A_j using eq. (12) and eq. (15) (or eq. (16). The objective function is to minimize the sum of square errors between "estimated" A_n and observed A_n (Simulation Error in Supplementary Material I). We calculated the real estimation errors after finishing the fitting procedure (True Error).

Yin et al. (2011b) gave the explicit results of RuBP carboxylation and PEPc carboxylation limited assimilation (AEE), RuBP carboxylation and PEPc regeneration limited assimilation (ATE), RuBP regeneration and PEPc carboxylation limited assimilation (AET) and RuBP regeneration and PEPc regneration limited assimilation (ATT). "Explicit" here means the assimilation rate are totally calculated by the estimated parameters without calculating the intermediates with observed A_n. The determination process of A_n is as follows:

$$\text{If } (V_{pc} < V_{pr}), A_c = AEE, A_j = AET, \text{otherwise } A_c = ATE, A_j = ATT \tag{23}$$

$$A_n = \min(A_c, A_j), \tag{24}$$

which we use for our estimation method (Supplementary Material II).

Checking inadmissible fits

We made it possible to check the inadmissible fits for limitation states in our estimation method (Supplementary Material I, II). After the estimation process finishes, the limitation states based on the estimated parameters will be calculated at the last column. If the calculated limitation states are inconsistent with the assigned ones in the estimation method, one needs to readjust the assignment of the "Estimate Limitation" (ajust CaL or CaH) and rerun the estimation method, until they are consistent with each other.

Temperature dependence of parameters or adjusting for temperature

In the models, K_c, K_o, V_{cmax}, V_{omax}, J_{max}, V_{pmax}, K_p, γ^* and g_m are temperature dependent (Table 1). K_c, K_o, V_{cmax}, J and γ^* follow the Arrhenius exponential functions (Bernacchi et al. 2001, 2003). V_{pmax} and g_m follow a bell-shaped model (Massad et al. 2007; Hardley et al. 1992; Bernacchi et al. 2002). K_p follows the Q_{10} function (Vico and Porporato 2008; Chen et al. 1994).

The temperature dependence equations for them are as follows:

$$K_o = K_o(25)e^{(c-\Delta H_a/(RT_k))} \tag{25}$$

$$K_c = K_c(25)e^{(c-\Delta H_a/(RT_k))} \tag{26}$$

$$V_{cmax} = V_{cmax}(25)e^{(c-\Delta H_a/(RT_k))} \tag{27}$$

$$\gamma^* = \gamma^*(25)e^{(c-\Delta H_a/(RT_k))} \tag{28}$$

$$J = J(25)e^{(c-\Delta H_a/(RT_k))} \tag{29}$$

$$V_{pmax} = \frac{e^{c-\Delta H_a/(RT_k)}}{1+e^{(\Delta S(T_l+273)-\Delta H_d)/R(T_l+273)}} \tag{30}$$

$$g_m = \frac{e^{c-\Delta H_a/(RT_k)}}{1+e^{(\Delta S(T_l+273)-\Delta H_d)/R(T_l+273)}} \tag{31}$$

$$K_p = K_p(25)Q_{10}^{T_k/(10-2.5)}, \tag{32}$$

where x(25) is the value of parameter at 25^oC, ΔH_a represents enthalpies of activation, R is the molar gas constant of 0.008314 $kJK^{-1}mol^{-1}$, T_k is the leaf temperature in K, ΔH_d is a term of deactivation and ΔS is a term of entropy and Q_{10} represents is a measure of the rate of change of a biological system as a consequence of increasing the temperature by 10 ^oC.

A/C_i curves can be measured at any temperature as long as the temperature remain constant during the measurements. The temperature dependence parameters are given (Table 1), based on which all the input parameters will be adjusted to the leaf temperatures at which A/C_i curves are measured . Then, using the temperature adjusted input parameters, the estimation method will first fit the output parameters at the leaf temperature and, further, calculate the output parameters at standard temperature (25 ^oC) based on the temperature response parameters of output parameters (Table 1). Since there are fewer studies that measure the temperature response parameters for C_4, we made the assumption that although the value of the parameters at standard temperature (25 ^oC)

(i.e. x(25)) change for C_4, the other temperature response parameters (i.e. ΔH_a, ΔH_d, ΔS and Q_{10}) are relatively conserved for C_3 and C_4. Parameters in Table 1 could be replaced with further measurements for C_4.

RESULTS

Estimation results and sensitivity analysis

Estimation methods based on the two equations of different assumptions about electron transport between RuBP regeneration and PEP carboxylation/regeneration yield consistent parameter estimates and assimilation-CO_2 response curves (Fig. 2, Supplementary material I and III), but there were minor differences. The second assumption that ATP, resulting from electron transport, is freely allocated between PEP carboxylation-regneration and RuBP regeneration leads to a bump at low low CO_2 when estimating A_j.The two assumptions produce different A_j under low CO_2; but this is largely inconsequential because under low CO_2, assimilation is usually limited by A_c.

The two fitting procedures also give similar estimation results with only slight differences (Supplementary material I and II). Yin et al.'s equation gives solutions with smaller overall error, but it is more sensitive to the limitation assignment, making it easy to get "unbalanced results" between Rubisco carboxylation and RuBP regeneration (Supplementary IV). Fig 3 shows an example of unbalanced simulation results using 10 Pa as CaL: A_c and A_j are similar at low C_i and one of them shows clear redundancy at high C_i.Thus, the range of variation in the transition point must be limited to a smaller range, say 20-50 Pa, for example. Sharkey et al.'s method is more robust with respect to balanced results, but it gives a slightly higher sum of error than Yin et al.'s method when unbalanced results are readjusted(Supplementary Material IV).

Our estimation methods assume the parameters, K_c, K_o, γ^*, K_p, α and g_{bs} to be constants; yet these parameters can vary widely in nature (Cousins et al. 2010) and it is therefore important to know how sensitive our results are to variation in these parameters. We conducted sensitivity analysis for variation in these parameters on the estimated V_{cmax}, J, R_d, V_{pmax} and g_m. Sensitivity analysis showed V_{cmax} and J are quite robust under the variation of K_c, K_o, γ^*, K_p, α and g_{bs}, while R_d, V_{pmax} and g_m were somewhat input dependent(Fig. 4). V_{pmax} is robust under all the other parameters except for the K_p. R_d and g_m show significant sensitivity to changes in K_p and to a lesser extent to K_c and g_{bs}. Thus, V_{cmax}, J and V_{pmax} are reliable from this estimation method. With external measurement methods as discussed in the following section, one can estimate more reliable R_d and g_m; supplementary Material V shows the how to change the Macro in Excel Solver.

Validation of the estimation methods

In order to test our estimation methods, we first conducted simulation test with manipulated error terms. We use the estimated parameters for our nine species to simulate new data sets using the C_4 photosynthesis equation based on the first assumption of electron transport and adding error terms to the assimilation rates. The error terms were randomly drawn from a normal distribution of mean zero and standard deviation of 0.1 or 0.2. Estimating simulated data sets gave us an idea about how likely we can capture the real parameters of the species given unavoidable errors in measurements. The results show that robust estimation results for V_{cmax}, J, V_{pmax} and R_d can be obtained. However, some estimation results of g_m show some deviation from the real values (Fig. 5).

To test whether our estimation method could give accurate predictions across typical prediction scenarios, (CO_2 ranging from 15 Pa to 65 Pa), we performed out of sample tests for our nine target species. To perform these tests, we removed five points of CO_2 concentrations between 15 and 65 Pa range out of the A/C_i curves and used the rest of the A/C_i curves to estimate parameters. And then we used these parameters to predict the assimilation rate under the CO_2 concentrations we took out before and further, calculated the estimation errors. In general, the estimation errors for all our species were small (Table 2).

Validating transition point range

We used chlorophyll fluorescence measurements from seven C_4 species to test whether the upper and lower boundary CO_2 concentrations, CaL and CaH, are reasonable (Table 3). Fluorescence analysis (Baker et al. 2007) is a powerful tool for identifying the limitation state of C_3 species (Sharkey et al. 2007). If Chlorophyll fluorescence is increasing with increasing CO_2, A_n is limited by Rubisco carboxylation limited; when Chlorophyll fluorescence stays constant with increasing CO_2, A_n is limited by RuBP regeneration. For C_4 species, however, the situation is more complicated. Since V_p could be limited by V_{pr} and V_{pc} (eq. (11)). Part of the RuBP carboxylation limited condition and RuBP regeneration limited condition will mix together, leading to a linear increase of fluorescence with increasing of CO_2, but of a very small slope. Thus, we can only obtain two boundary CO_2 concentrations. Below the lower boundary, A_n is Rubisco carboxylation limited; above the higher boundary, A_n is RuBP regeneration limited. We measured fluorescence to test whether the upper and lower boundary CO_2 concentrations, CaL and CaH, are reasonable. Most of the CaL are above 15 Pa (lowest is around 14 Pa) and all the CaH are below 65 Pa. These results suggest that 15Pa-65Pa is a reasonable range to start with.

DISCUSSION

The photosynthetic parameters from the estimation method are good indicators for the biochemical and biophysical mechanisms underlying the photosynthesis processes of plants. Together with photosynthesis models, they can provide powerful information for evolutionary and ecological questions, as well as in efforts to improve crop productivity (Osborne & Beerling, 2006; Heckmann et al. 2013). Photosynthetic parameters represent different physiological traits, and comparison of these parameters within a phylogenetic background could help us to understand the further divergence of lineages and species through evolutionary time. Additionally, the response of productivity and carbon cycle of vegetation towards the future climate change depends heavily on photosynthesis parameter estimation.

Our estimation method shares with previous methods an underlying assumption that dark and light reactions optimally co-limit the assimilation rate (Sharkey et al. 2007; Yin et al. 2011b; Ubierna et al. 2013; Bellasio et al. 2015). This requires that there is some kind of optimization of nitrogen allocation of Rubisco carboxylation and RuBP regeneration. In our estimation method, we relax the optimization assumption to the extent that the transition point will be estimated instead of being assigned in advance. The optimality assumption is intuitive when we are considering there should be some mechanism to balance the resource distribution between dark and light reaction to avoid inefficiency. However, it is still possible that there is redundancy in nitrogen allocation in one reaction, which can cause the photosynthesis rate to be always limited by the dark or light reactions.

Our results show that despite a clear difference between the assumptions of how the products

of electron transport are distributed, the results are similar to each other, and comparable with studies using different models under measurements of high light intensity. However, under lower light intensity, assimilation rate will be limited more by A_j, and the two assumptions may start to show divergent results. In addition, since the fluorescence curves (Fig. 5), which represent the electron transport, do not show a transient bump, the first assumption should be more reliable.

Each of the two different fitting procedures has advantages and disadvantages. Yin's method uses the explicit calculation of assimilation rate, and consequently gives lower estimation error. However, it needs a more accurate assignment of limitation states, especially at the lower end. Thus, Yin's method will be preferable if one has additional support (e.g. fluorescence measurement) to define the limitation states; otherwise the Yin's method may give unbalanced results (Fig. 4). However, Sharkey's method usually can avoid unbalanced resutls even without ancillary measurements. Thus, it is better to use both procedures to support each other to find more accurate results. For example, one can first use Sharkey's method to get estimation results and limitation states, and then use them as initial values for Yin's method.

Although we have shown that parameter estimation can be achieved solely with A/C_i curves, it is easy to combine our methods with ancillary measurements to yield more accurate estimation results by defining the parameters as estimated or known (Supplementary Material V). Chlorophyll fluorescence analysis discussed above is one potential external measurement. With reliable measurement of leaf absorptance (a), chlorophyll fluorescence could be used to get quantum yield (ϕ_{PSII}) and to independently estimate electron transport rate (J) by eq. (33):

$$J = \phi_{PSII} \times a \times I \times 0.5, \tag{33}$$

where I is the light intensity and 0.5 means partitioning of energy between PSI and PSII is

equivalent. However, in order to use fluorescence to estimate J for C_4 species, the equation, leaf absorptance and energy partition between PSI and PSII should all be verified first for C_4 species. Yin et al. (2011b) propose a method to obtain R_d from the fluorescence-light curve, since the method used for C_3 species, the Laisk method, is inappropriate (Yin et al. 2011a). Yin et al. (2011b) and Bellasio et al. (2015) also proposed methods to measure J using the fluorescence-light curves under regular (20%) and low (2%) O_2 concentration. Flexas et al. (2007) discussed the estimation method of g_m for C_3 species using the instantaneous carbon isotope discrimination, which could be generalized to estimate g_m for C_4 species. With external measurement results, one can change estimated parameters (such as R_d, g_m and J) as input parameters in this curve fitting method. Furthermore, if R_d, g_m or J are determined in the external measurements, one can also relax the input parameters (such as g_{bs}) and make them as estimated parameters (Supplementary material V).

In this study, we present new accessible estimation tools for extracting C_4 photosynthesis parameters from intensive A/C_i curves. Our estimation method is based on established estimation method for C_3 plants and makes several improvements upon C_4 photosynthesis models. External measurements for specific parameters will increase the reliability of estimation methods and are summarized independently. We tested two assumptions related to whether the electron transport is freely distributed between RuBP regeneration and PEP regeneration or certain proportions are confined to the two mechanisms. They show similar results under high light, but they may divergence under low light intensities. The two fitting procedures have distinct advantages and disadvantages and could be mutually supportive. Simulation test, out of sample test, fluorescence analysis and sensitivity analysis confirmed that our methods gave robust estimation especially for

V_{cmax}, J and V_{pmax}.

ACKNOWLEDGMENT

We sincerely thank Dr. Jesse Nippert, Kansas State University, for providing the fluorometer chamber for the measurement.

The list of supplementary material

Supplementary Material I. The estimation method of model 1 using Sharkey's fitting procedure.

Supplementary Material II. The estimation method of model 1 using Yin's fitting procedure.

Supplementary Material III. The estimation method of model 2 using Sharkey's fitting procedure.

Supplementary Material IV. Estimation results under CaL of 10 Pa or changing CaL to avoid the unbalanced estimated A_c and A_j.

Supplementary Material V. Instruction for use and set the solver macro.

Supplementary Material Table S1. Parameter abbreviation.

C4Estimation_0.1.tar.gz is the R package which contains estimation methods of Sharkey's and Yin's procedures for model 1.

REFERENCES

Baker N.R., Harbinson J. & Kramer D.M. (2007) Determining the limitations and regulation of photosynthetic energy transduction in leaves. *Plant, Cell and Environment* 30, 1107–1125.

Bellasio C., Beerling D.J. & Griffiths H. (2015) Deriving C_4 photosynthetic parameters from combined gas exchange and chlorophyll fluorescence using an Excel tool: theory and practice. *Plant, Cell and Environment* doi: 10.1111/pce.12626.

Bernacchi C.J., Singsaas E.L., Pimentel C., Portis A.R. & Long S.P. (2001) Improved temperature response functions for models of Rubisco-limited photosynthesis. *Plant, Cell and Environment* 24, 253–259.

Bernacchi C.J., Portis A.R., Nakano H., von Caemmerer S. & Long S.P. (2002) Temperature response of mesophyll conductance. Implications for the determination of Rubisco enzyme kinetics and for limitatins to photosynthesis in vivo. *Plant Physiology* 130, 1992-1998.

Bernacchi C.J., Pimentel C. & Long S.P. (2003) In vivo temperature response functions of parameters required to model RuBP-limited photosynthesis. *Plant, Cell and Environment* 26, 1419-1430.

Von Caemmerer S. (2000) Biochemical models of photosynthesis. In Techniques in Plant Sciences p. 196. CSIRO Publishing, Colingwood, Australia.

Chen D.-X., Coughenour M.B., Knapp A.K. & Owensby C.E. (1994) Mathematical simulation of C_4 grass photosynthesis in ambient and elevated CO_2. *Ecological Modelling* 73, 63–80.

Cousins A.B., Ghannoum O., von Caemmerer S. & Badger M.R. (2010) Simultaneous determination of Rubisco carboxylase and oxygenase kinetic parameters in *Triticum aestivum* and *Zea mays* using membrane inlet mass spectrometry. *Plant, Cell and Environment* 33, 444–452.

Dubois J.B., Fiscus E.L., Booker F.L., Flowers M.D. & Reid C.D.(2007) Optimizing the statistical estimation of the parameters of the Farquhar-von Caemmerer-Berry model of photosynthesis. *New Phytologist* 176, 402–414.

Ethier G.J., Livingston N.J., Harrison D.L., Black T.A. & Moran J.A. (2006) Low stomatal and internal conductance to CO_2 versus Rubisco deactivation as determinants of the photosynthetic decline of ageing evergreen leaves. *Plant, Cell and Environment* 29, 2168-2184.

Farquhar G.D., Von Caemmerer S. & Berry J.A. (1980) A biochemical model of photosynthetic carbon dioxide assimilation in leaves of 3-carbon pathway species. *Planta* 149, 78-90.

Flexas J., Diaz-Espejo A., Galmés J., Kaidenhoff R., Medrano H. & Ribas-Carbo M. (2007) Rapid variations of mesophyll conductance in response to changes in CO_2 concentration around leaves. *Plant, Cell and Environment* 30, 1284-1298.

Gu L., Pallardy S.G., Tu K., Law B.E. & Wullschleger S.D. (2010) Reliable estimation of biochemical parameters from C_3 leaf photosynthesis-intercellular carbon dioxide response curves. *Plant, Cell and Environment* 33, 1852-1874.

Hatch M.D. (1987). C_4 photosynthesis: a unique blend of modified biochemistry, anatomy and ultrastructure. *Biochimica et Biophysica Acta* 895, 81-106.

Hardley P.C., Thomas R.B., Reynolds J.F. & Strain B.R. (1992) Modelling photosynthesis of cotton grown in elevated CO_2. *Plant, Cell and Environment* 15, 271-282.

Heckmann D., Schulze S., Denton A., Gowik U., Westhoff P., Weber A.P. & Lercher M.J. (2013) Predicting C_4 photosynthesis evolution: Modular, individually adaptive steps on a Mount Fuji fitness landscape. *Cell* 153, 1579-1588.

Miao Z.W., Xu M., Lathrop R.G. & Wang Y.F. (2009) Comparison of the A-C_c curve fitting methods in determining maximum ribulose 1.5-bisphosphate carboxylase/oxygenase carboxylation rate, potential light saturated electron transport rate and leaf dark respiration. *Plant, Cell and Environment* 32, 1191-1204.

Massad R. S., Tuzet A. & Bethenod O. (2007) The effect of temperature on C_4-type leaf photosynthesis parameters. *Plant, Cell and Environment* 30, 109-122.

Osborne C.P. & Beerling D.J. (2006) Nature's green revolution: the remarkable evolutionary rise of C-4 plants. *Philosophical Transactions of The Royal Society B* 361, 173-194.

Osborne C.P. & Sack L. (2012) Evolution of C4 plants: a new hypothesis for an interaction of CO2 and water relations mediated by plant hydraulics. *Philosophical Transactions of The Royal Society B* 367, 583-600.

Sharkey T.D., Bernacchi C.J., Farquhar G.D. & Singsaas E.L. (2007) Fitting photosynthetic carbon dioxide response curves for C3 leaves. *Plant, Cell and Environment* 30, 1035–1040.

Ubierna N., Sun W., Kramer D.M. & Cousins A.B. (2013) The efficiency of C_4 photosynthesis

under low light conditions in Zea mays, Miscanthus X giganteus and Flaveria bidentis. *Plant, Cell and Environment* 36, 365-381.

Vico G. & Porporato A. (2008) Modelling C_3 and C_4 photosynthesis under water-stressed conditions. *Plant and Soil* 313, 187-203.

Xu L.K. & Baldocchi D.D. (2003) Seasonal trends in photosynthetic parameters and stomatal conductance of blue oak (*Quercus douglasii*) under prolonged summer drought and high temperature. *Tree Physiology* 23, 865-877.

Yin X., Struik P.C., Romero P., Harbinson J., Evers J.B., Van Der Putten P.E.L. & Vos J.A.N. (2009) Using combined measurements of gas exchange and chlorophyll fluorescence to estimate parameters of a biochemical C_3 photosynthesis model: a critical appraisal and a new integrated approach applied to leaves in a wheat (*Triticum aestivum*) canopy. *Plant, Cell and Environment* 32, 448-464.

Yin X., Sun Z., Struik P.C. & Gu J. (2011a) Evaluating a new method to estimate the rate of leaf respiration in the light by analysis of combined gas exchange and chlorophyll fluorescence measurements. *Journal of ExperimentalBotany* 62, 3489-3499.

Yin X.Y., Sun Z.P., Struik P.C., Van der Putten P.E.L., Van Ieperen W. & Harbinson J. (2011b) Using a biochemical C4 photosynthesis model and combined gas exchange and chlorophyll fluorescence measurements to estimate bundle-sheath conductance of maize leaves differing in age and nitrogen content. *Plant, Cell and Environment* 34, 2183-2199.

Table 1. Temperature dependence of photosynthesis parameters.

	25°C	c	$\Delta H_a/Q_{10}$	ΔH_d	ΔS
Input parameters adjustment					
K_c(Pa)	65[a]	36.8472	80.99[b]		
K_o(kPa)	45[a]	13.3757	23.72[b]		
γ*	0.000193[a]	1.3148	24.46[b]		
K_p(Pa)	8[a]	2.629	2.1[c]		
Output parameters adjustment					
V_{cmax} (µmol m^{-2} s^{-1})		26.355	65.33[b]		
J (µmol m^{-2} s^{-1})		17.71	43.9[d]		
TPU (µmol m^{-2} s^{-1})		21.46	53.1[e]	201.8[e]	0.65[e]
V_{pmax} (µmol m^{-2} s^{-1})		29.393	70.37[f]	117.9[f]	0.4[f]
R_d (µmol m^{-2} s^{-1})		18.715	46.39[b]		
g_m(µmol m^{-2} $s^{-1}$$Pa^{-1}$)		20.01	49.6[g]	437.4[g]	1.4[g]

c (scaling constant), ΔH_a (enthalpies of activation), ΔH_d (enthalpies of deactivation), ΔS (entropy) and Q_{10} (rate of change as a consequence of increasing the temperature by 10°C, for K_p) are parameters for temperature response of photosynthesis parameters. K_c, Michaelis-Menten constant of Rubisco activity for CO_2; K_o, Michaelis-Menten constant of Rubisco activity for O_2; γ*, specificity of Rubisco; K_p, Michaelis-Menten constant of PEPc activity for CO_2; V_{cmax}, maximal velocity of carboxylation for Rubisco; *J*, rate of electron transport; *TPU*, triose phosphate use; V_{cmax}, maximal velocity of carboxylation for PEPc; R_d, mitochondrial respiration rate in the daytime; g_m, mesophyll conductance.

[a]von Caemmerer (2000), [b]Bernacchi et al.(2001), [c]Chen et al.,1994, [d]Bernacchi et al.(2003), [e]Hardley et al. (1992), [f]Massad et al. (2007),[g]Bernacchi et al.(2002)

Table 2. Out of sample test results. Five measured points from 15 Pa-65 Pa were taken out when we conducted the estimation process. Then the calculated assimilation rates under these five CO_2 concentrations were compared with the measured ones. The data shows difference between the calculated and measured assimilation rates (mean(standard error) with unit $\mu mol\ m^{-2}\ s^{-1}$).

Species	*A. virginicus*	*Z. mays*	*E. trichodes*	*S. scoparium*	*P. virgatum*
Sharkey's method	-0.115 (0.056)	0.075(0.121)	0.018 (0.059)	-0.302 (0.071)	0.098(0.091)
Yin's method	-0.128(0.056)	-0.104(0.083)	0.003 (0.059)	-0.013(0.071)	0.018(0.091)
Species	*P. amarum*	*S. faberi*	*S. nutans*	*T. dactyloides*	
Sharkey's method	-0.135(0.077)	-0.109(0.056)	-0.103(0.069)	-0.105(0.102)	
Yin's method	-0.102(0.076)	-0.115(0.056)	-0.043(0.069)	-0.095(0.102)	

Table 3. CO_2 concentration boundaries results for assimilation limited conditions from fluorescence measurements for seven species. CaL: CO_2 concentration under which assimilation rate is limited by Rubisco carboxylation. CaH: CO_2 concentration under which assimilation rate is limited by RuBP regeneration.

Species	*P. virgatum*	*P. amarum*	*S. scoparium*	*S. nutans*
CaL(Pa)	14.1(1.12)	18.0(1.09)	17.8(1.09)	17.6(0.28)
CaH(Pa)	34.1(1.78)	55.5(1.40)	53.1(1.10)	63.1(2.07)

Species	*T. dactyloides*	*T. flavus*	*B. mutica*
CaL(Pa)	13.8(0.35)	14.9(2.35)	15.8(1.13)
CaH(Pa)	46.1(0.20)	41.4(1.73)	42.3(1.24)

Figure Captions

Fig. 1. An introduction of how our estimation method assigns transition points between limitation states. A_c represents RuBP carboxylation limited assimilation rate, A_j represents RuBP regeneration limited assimilation rate. Transition point is given by the interaction of the A_c and A_j curves. Our algorithm allows the transition point to vary from a lower bound (CaL, 15 Pa for example) and a higher bound (CaH, 65 Pa for example), indicated by the dashed vertical lines in the figure.

Fig. 2. Assimilation-CO_2 response curves (A/C_i) generated using C_4 photosynthesis of two different assumptions. Photosynthetic parameters (V_{cmax}, J, R_d, V_{pmax} and g_m) are the same for both assumptions. A_c represents RuBP carboxylation limited assimilation, A_j_Assumption 1 represents results of the assumption that no matter how much electron transport is used for PEP carboxylation/regeneration, a certain amount (xJ) is confined for this use, and A_j_Aassumption 2 represents results of the assumption that electron transport can be freely distributed between PEP carboxylation/regeneration and RuBP regeneration. Parameters are estimated from A/C_i curve of *Schizachyrium scoparium* (Michx.) Nash under light intensity of 1500 μmol m^{-2} s^{-1}. The figure shows that although the models for A_j differ at low CO_2 concentrations, this difference is inconsequential, because the assimilation rate is limited by A_c at that range.

Fig. 3. An example of unbalanced results by using 10 Pa as CaL in estimation method. Compare estimated results (A_c and A_j) using Yin's estimation method with CaL of 10 Pa and 15 Pa and observed A (A_{obs}) under different C_i concentrations. The data are from *Eragrostis trichodes* (Nutt.) Alph. Wood under light intensity of 1500 μmol m^{-2} s^{-1}. The estimated A is the minimum of A_c and A_j.

Fig. 4. Sensitivity analysis of five estimation parameters to the variation in six input parameters. Relative changes in the estimated V_{cmax}, J, R_d, V_{pmax} and g_m in response to

the relative change of six input parameters [(a) α, (b) K_p, (c) K_o, (d) K_c, (e) γ^* and (f) g_{bs}] from the initial values in Table 1. The relative change of estimated parameters refers to the ratio of estimated values at a changed input parameter to the estimated value at the initial value of that input parameter. The symbols represent the average change of the ten C_4 species and error bars stand for standard error.

Fig. 5. Simulation tests for the estimated parameters using estimation methods of Yin's and Sharkey's fitting procedures. Data sets are generated by adding random errors for the modeling results using the known photosynthesis parameters of nine species. Small error refers to error term randomly chosen with mean 0 and standard deviation of 0.1 and bigger error refers to error term with randomly chosen mean 0 and standard deviation of 0.2.

Fig. 6. Quantum yield calculated from fluorescence measurement for two species. Dots represent *P. amarum* and diamonds represent *T. flavus*. Black dots/diamonds: Rubisco carboxylation limitated states; grey dots/diamonds: co-limitated states; open dots/diamonds: RuBP regeneration regeneration limited states.

Fig. 1

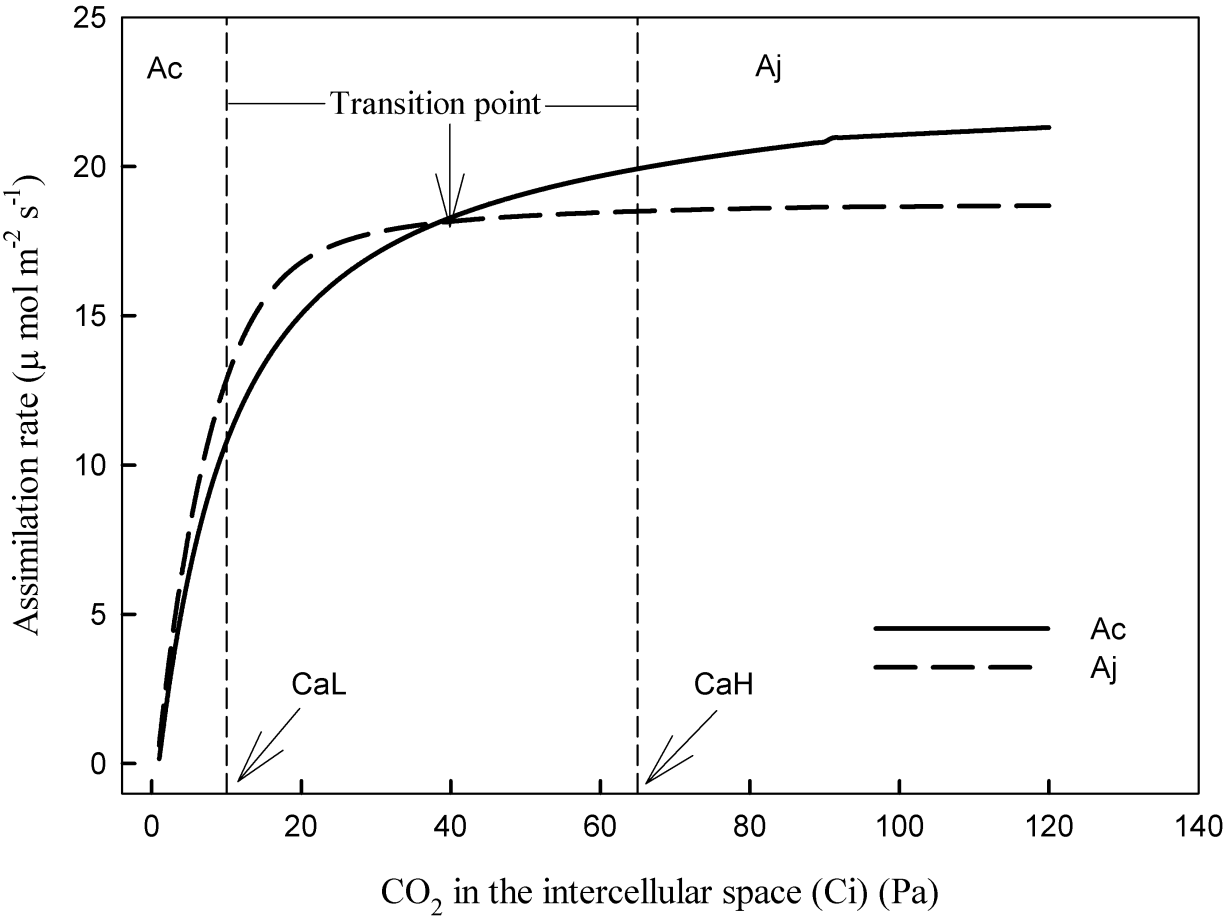

Fig. 2

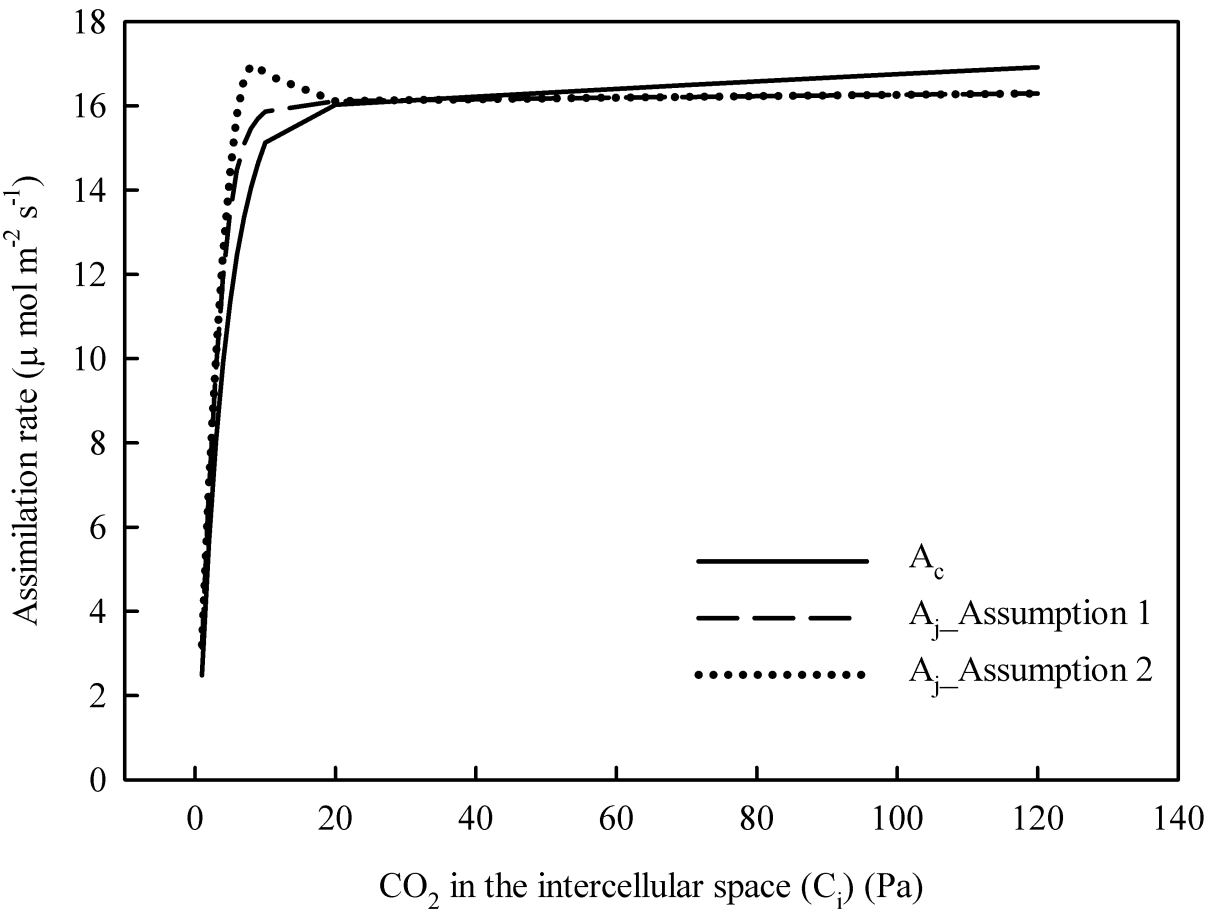

Fig. 3

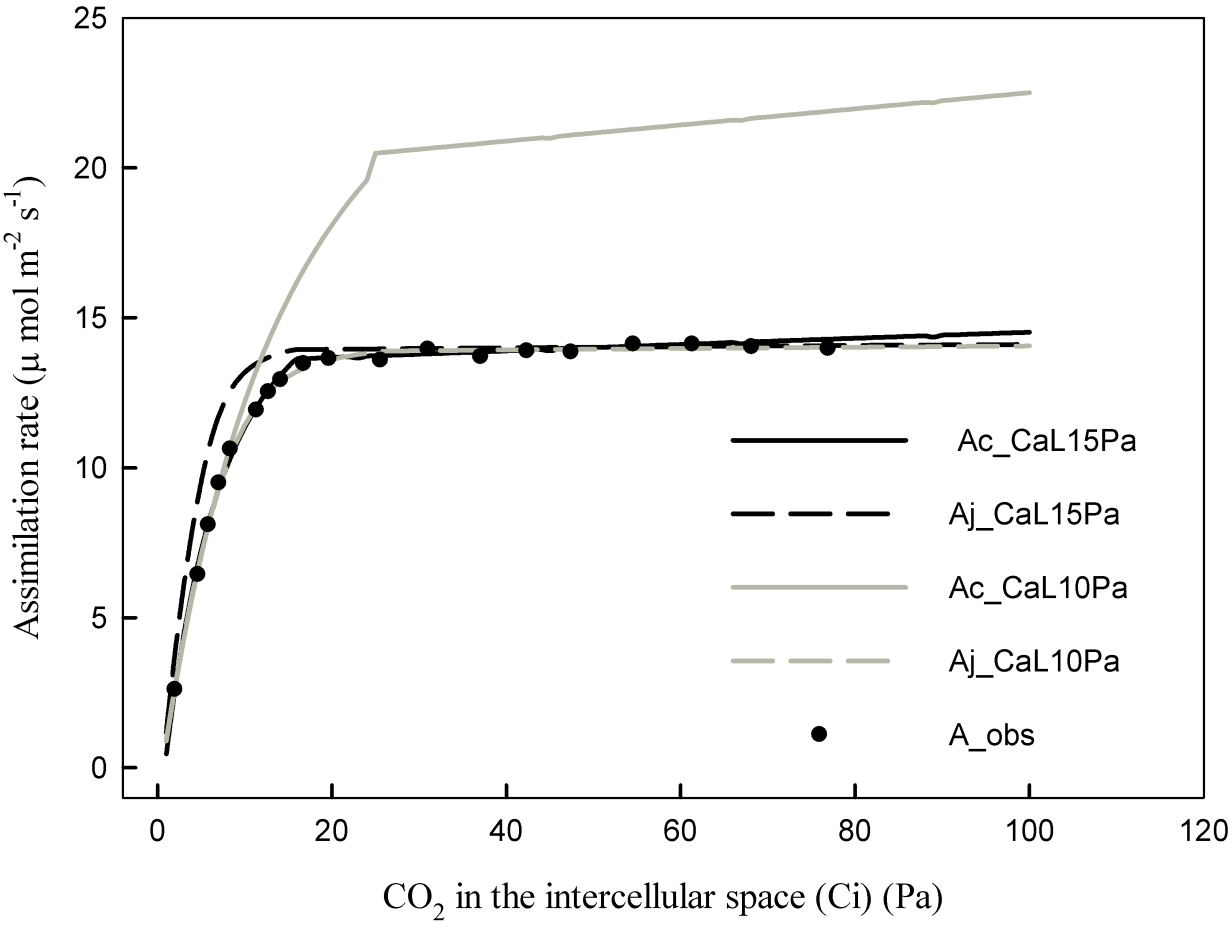

Fig. 4

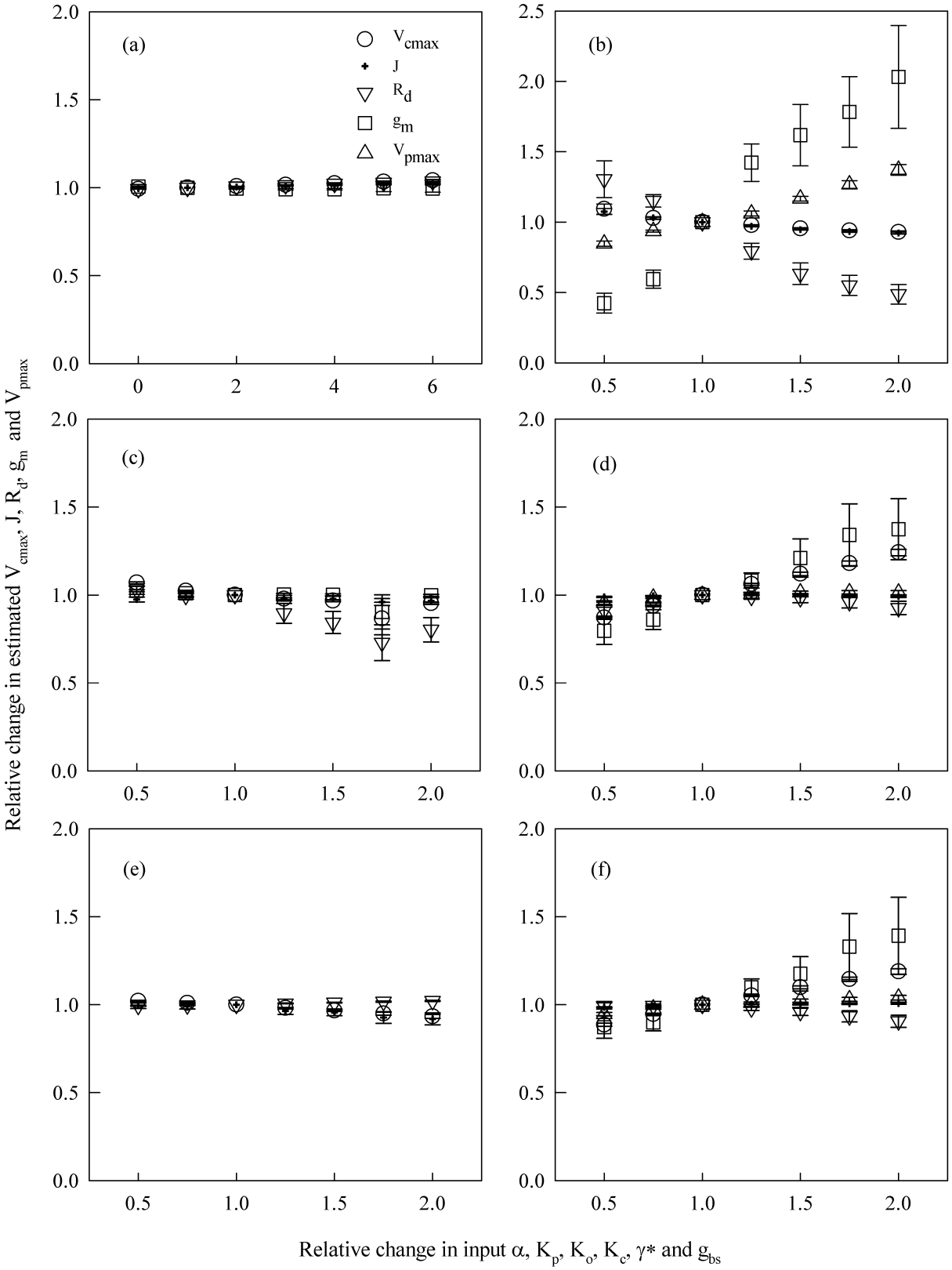

Fig. 5

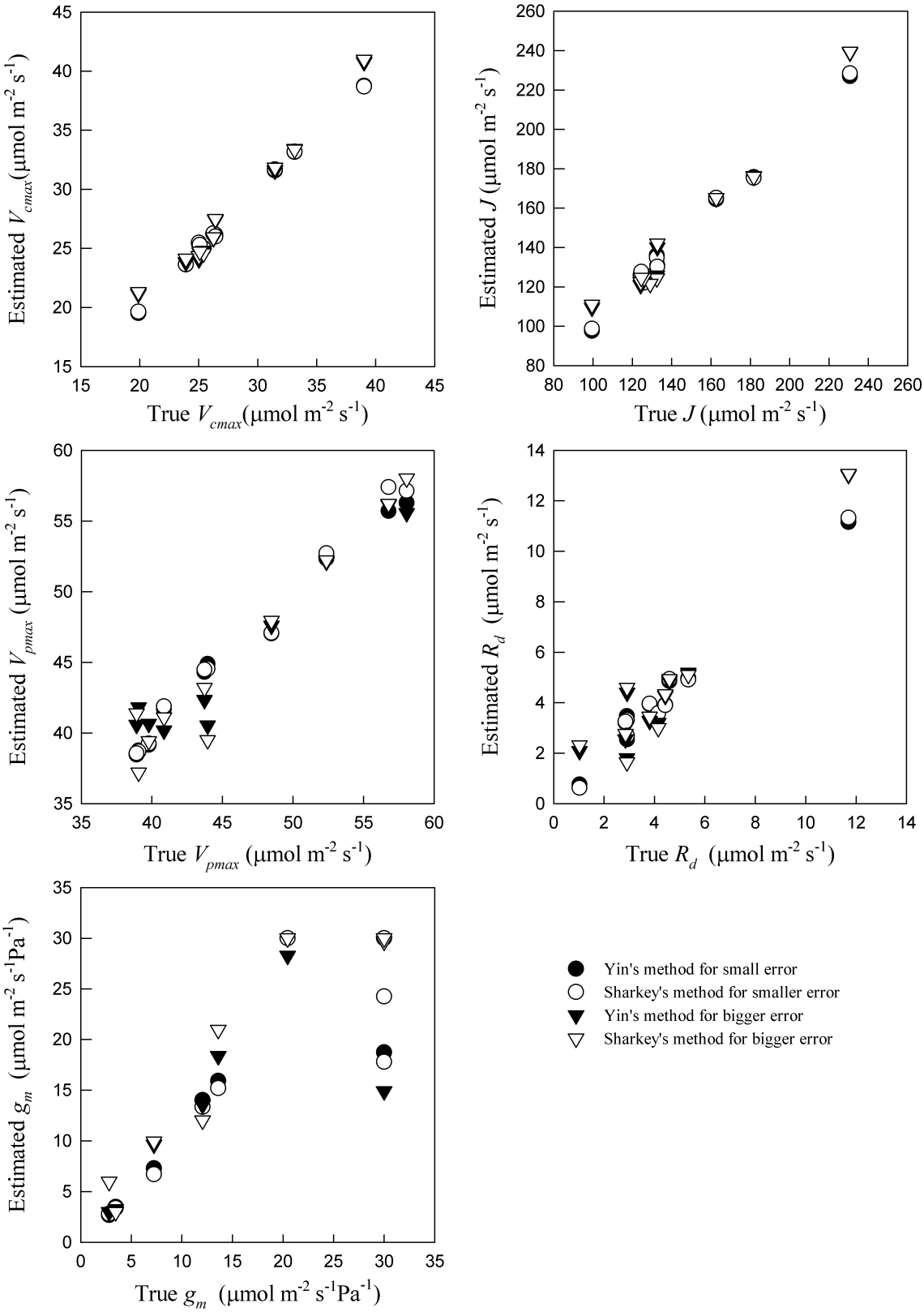

Fig. 6